

**Suppressed surface alloying for a bulk miscible system: Ge on Pt(100)**Matthias Batzill,<sup>\*</sup> Taketoshi Matsumoto, Chi-Sung Ho, and Bruce E. Koel<sup>†</sup>*Department of Chemistry, University of Southern California, Los Angeles, California 90089, USA*

(Received 18 November 2003; published 16 March 2004)

Structural characterization by scanning tunneling microscopy and alkali low-energy ion scattering spectroscopy of Pt(100) surfaces covered by less than 0.5-ML Ge is reported. Despite bulk solubility of Ge in Pt, it was found that Ge remains on top of the Pt(100) surface as adatoms even after annealing to 1200 K. Furthermore, Pt adatoms produced by lifting of the Pt(100)-hex reconstruction in the vicinity of adsorbed Ge do not intermix with the Ge but rather segregate to form pure-Pt islands with Ge adsorbed on top. Ge adatoms disperse across the surface and form a disordered adlayer at low coverages. We propose that this is because of a significant charge transfer from the substrate to the adsorbate which causes a dipole-dipole repulsive interaction between the Ge adatoms. At a coverage of 0.5-ML Ge, an ordered  $c(2\times 2)$ -Ge adlayer forms.

DOI: 10.1103/PhysRevB.69.113401

PACS number(s): 68.35.Bs, 61.66.Dk, 61.18.Bn

**I. INTRODUCTION**

The performance of supported-Pt heterogeneous catalysts are often improved by the addition of a second metal component. Common additives are Sn, Re, Ru, Pb, Zn, Al, Ga, Ir, Cr, and Ge.<sup>1-4</sup> In many cases, the metal salts are reduced and combine with Pt to form bimetallic alloy clusters.<sup>5,6</sup> Fundamental surface science studies on well-defined single crystal surfaces are helpful in understanding this alloying process and the structure of the alloy clusters.

Characterization of the surface structure and composition for several crystallographic faces within the same alloy system enables us to gain a better understanding of the origin of the altered chemical properties of bimetallic clusters in supported catalysts. Recently, the alloying of Ge with the Pt(111) surface was investigated. A  $5\times 5$  unit cell was reported by Fukutani *et al.*<sup>7</sup> Studies in our laboratory established a similarly large, but different, unit cell with a  $(\sqrt{19}\times\sqrt{19})R23.4^\circ$  structure and one Ge atom per unit cell.<sup>8</sup> On Pt(111), the addition of even low concentrations of Ge alters the chemical properties of the surface.<sup>9-12</sup>

Herein, investigations of the Ge/Pt(100) system are reported. We found that Ge alloying is suppressed for low Ge coverages on this surface. It is well established that differences in surface energies and the degree of misfit between the substrate and deposited elements can alter alloy formation at surfaces. This may cause alloying at surfaces of bulk-immiscible elements.<sup>13-16</sup> The opposite effect, that bulk-miscible elements show a suppressed alloying at surfaces, has not previously been reported to our knowledge, but is described in this paper.

**II. EXPERIMENTAL METHODS**

The experiments reported here were performed in two ultrahigh vacuum chambers. Detailed descriptions of the scanning tunneling microscopy (STM) chamber and alkali low-energy ion scattering spectroscopy (ALISS) chamber can be found elsewhere.<sup>17,18</sup>

The Pt sample was cleaned by cycles of 500-eV Ar<sup>+</sup> ion sputtering, and then annealing in  $5\times 10^{-7}$ -Torr O<sub>2</sub> with the

sample at 1000 K, and finally annealing in vacuum with the sample at 1200 K. This procedure resulted in the characteristic low energy electron diffraction (LEED) pattern for the hex-reconstructed Pt(100) surface and no contamination at the surface was detected by Auger electron spectroscopy in the STM chamber or by x-ray photoelectron spectroscopy in the ALISS chamber. The same Pt(100) single crystal was used in both chambers.

Ge was evaporated from a resistively heated Ta boat and deposited on the sample at room temperature. The sample was subsequently annealed to a target temperature and then examined by STM or ALISS at room temperature. The sample temperature was measured by a chromel/alumel thermocouple directly spot-welded to the side of the crystal. Incident 1-keV Li<sup>+</sup> ions were used for ALISS experiments. Ge coverages reported herein were estimated by defining  $\theta_{\text{Ge}} = 0.5$  ML as the minimum amount of Ge that was necessary to deposit in order to form a  $c(2\times 2)$ -Ge structure covering the entire surface following annealing.

**III. RESULTS AND DISCUSSION**

Figure 1 shows representative STM images for low coverages of Ge (below 0.3 ML) annealed to 600 K for 10 s. Pure-Pt regions, visible as hex-reconstructed areas [marked 1a in Fig. 1(a)] remain at such low Ge coverages for short annealing times at moderate temperatures. Repeatedly imaging the same area with the STM modified these hex-reconstructed domains to form areas identified as structure 1b in Fig. 1(a). Such a tip induced restructuring of the surface has never been observed on the clean Pt(100)-hex surfaces. It is known that in order to lift the hex-reconstruction more than one adsorbate atom/molecule is required,<sup>19</sup> i.e., a single Ge atom does not lift the reconstruction. Furthermore, it has been observed that metal adatoms can diffuse over 10–100 nm on the reconstructed surface before nucleating an adisland at room temperature.<sup>20</sup> Thus we propose that mobile Ge atoms are present on the hex-reconstructed domains and that these adatoms can lift the reconstruction in the presence of strong electric field of the STM tip. For the purpose of a further discussion, however, it is only important to note that

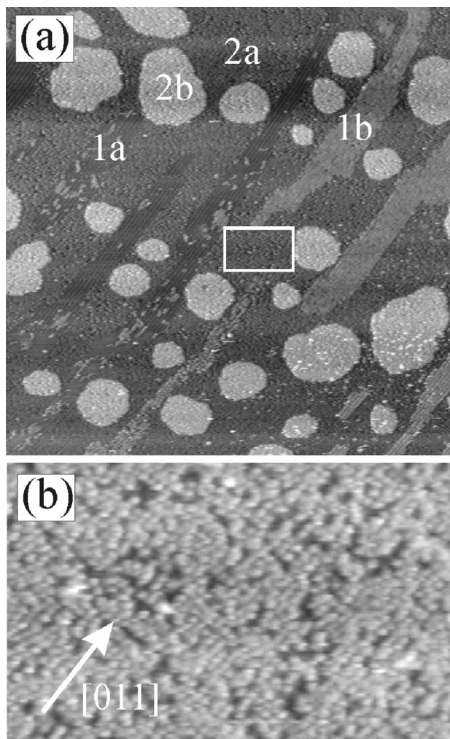


FIG. 1. STM images of sub-0.3-ML Ge coverage on a Pt(100) surface annealed to 600 K. (a) Image size  $(150 \text{ nm})^2$ ,  $V_{\text{Bias}} = 115 \text{ mV}$ , and  $I = 0.27 \text{ nA}$ . Four surface structures are distinguished: 1a for hex-reconstructed areas, 1b for hex-reconstructed areas modified by the action of the STM tip, 2a for Ge covered Pt terraces, and 2b for Ge covered Pt adislands. (b) Zoomed-in area marked in (a); image size  $27 \times 18 \text{ nm}^2$ ,  $V_{\text{Bias}} = 115 \text{ mV}$ , and  $I = 0.23 \text{ nA}$ .

1b-type regions were reconstructed previous to the tip-induced restructuring. 1a- and 1b-type regions, are easily distinguished in the STM images from the remaining surface areas and thus the fraction of the surface that remained hex-reconstructed after sample preparation can be easily measured. The main mesoscopic features in these remaining areas are Ge adlayer regions [2a in Fig. 1(a)] and compact islands [2b in Fig. 1(a)] that are tens of nanometers in diameter and  $\sim 0.2 \text{ nm}$  in height, which corresponds well to height of a single monatomic step of the Pt(100) surface. These islands cover  $22 \pm 2\%$  of the surface area, excluding hex-reconstructed domains, i.e., 1a- and 1b-type areas in Fig. 1. This island coverage is equal to the amount of Pt that is “expelled” from the surface layer upon lifting of the hex-reconstruction by Ge adsorption, i.e., the hex-reconstructed surface density is  $\sim 20\%$  higher than the bulk-terminated (100) plane of Pt. Therefore it can be concluded from STM images that the expelled Pt adatoms agglomerate to form pure-Pt adislands, and this indicates that Ge and Pt do not alloy even if they are available as atomically dispersed adatoms at the Pt(100) surface.

Atom-size protrusions are imaged in STM on top of the terraces [Fig. 1(b)] and also on top of the adislands. These protrusions have an apparent height of  $0.1\text{--}0.15 \text{ nm}$ , in areas where they are spaced far enough for the STM tip to pen-

etrate to the substrate, and align preferentially along the [011] azimuth of the Pt substrate. These protrusions are associated with Ge atoms that are separated by distances much greater than close packing. Thus, Ge atomically disperses across the surface and so does not behave like other metal-on-metal epitaxial-growth systems where compact adislands are formed with interatomic spacings of either the bulk metal or substrate periodicity.

If this surface is annealed to temperatures higher than 600 K, any pure-Pt hex-reconstructed domains disappear completely in the STM images, in agreement with LEED observations that showed only  $1 \times 1$  diffraction spots. The adislands also disappear because of migration and coalescence of the adislands to form larger terraces. Annealing even to 1200 K (the limit in our experimental setup) did not reform a hex-reconstructed surface as one would expect if Ge diffused into the bulk or evaporated from the surface.

Further discussion of the growth of Ge on Pt(100) at room temperature and the structure of surfaces that contain higher Ge coverages (above 0.5 ML) will be discussed in detail in another communication.<sup>21</sup> Here, we only mention that deposition of excess 0.5-ML Ge results in an ordered Ge overlayer with a  $c(2 \times 2)$  LEED pattern upon annealing to 700 K. The excess Ge that is not consumed in the overlayer diffuses into the bulk of the Pt crystal.

In order to exclude ambiguities inherent in STM, such as tip-induced surface restructuring and apparent contrast effects that can make a distinction between alloy and overlayer phases difficult, ALISS was employed to substantiate the structural model inferred by the above-described STM studies. A description of the structural determination by ion scattering spectroscopy can be found for example in Ref. 22. Peaks for Pt and Ge scattering were monitored and polar angle scans were taken along the [010] and [011] azimuthal orientations of the Pt(100) crystal. The angular intensities carry much information, but for the purpose here we can simply determine the critical polar angle for the onset of enhanced ion scattering, i.e., the ion incidence angle at which substrate atoms emerge out of the ion shadow-cone region caused by their neighboring atoms. For atom arranged in a plane, a smaller critical angle is indicative of a longer separation between atoms. Therefore, an overlayer with a longer separation between atoms as is suggested by the STM data can be easily discriminated from an incorporated alloy structure (for a transformation from an overlayer to an alloy see, for example, Ref. 23) in which Ge atoms occupy lattice sites in the top Pt layer with Pt-Ge separation close to the Pt(100)- $(1 \times 1)$  atom separation by measuring the critical angle. Figure 2 presents ALISS polar scans after a Ge coverage of 0.5 ML was annealed to 900 K to produce a sharp  $c(2 \times 2)$  LEED pattern [(a) and (c)] and a Ge coverage of 0.2 ML was annealed to 600 K, which is similar to the preparation of the sample prior to obtaining the STM images shown above [(b) and (d)]. Two features arise in these curves, one at relatively low angles near  $20^\circ$  due to scattering from atoms in the surface plane and another at higher angles near  $70^\circ$  due to scattering from second-layer atoms. Figure 2(a) shows similar critical angles for Ge and Pt scattering in the first layer along the [010] azimuth, although it is consistently

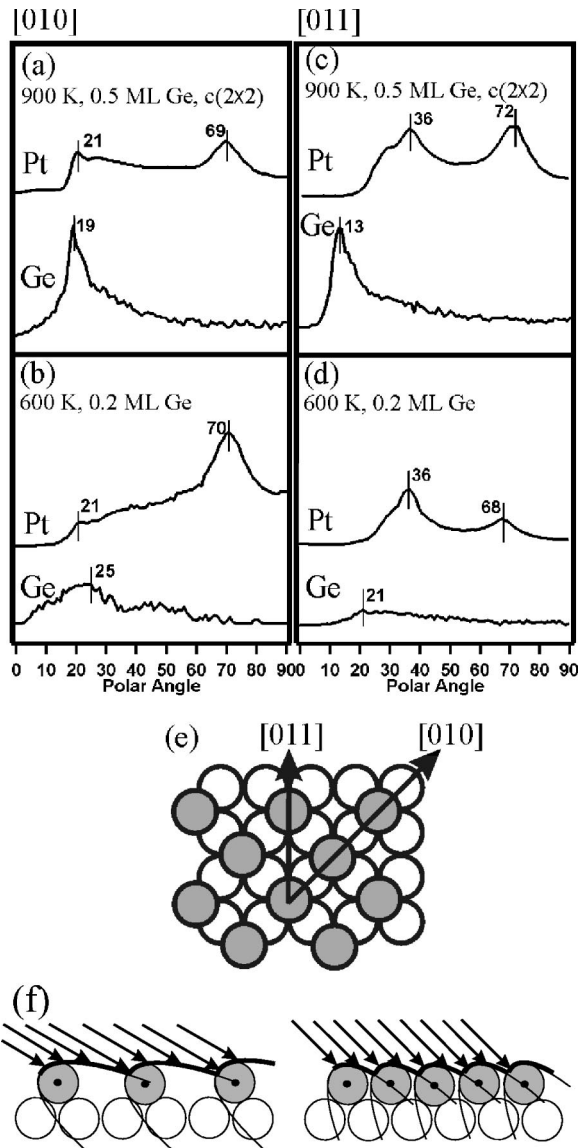


FIG. 2. ALISS polar scans for Pt and Ge along the [010] azimuth [left panel, (a) and (b)], and along the [011] azimuth [right panel, (c) and (d)]. Two samples were examined. One sample had slightly more than 0.5 ML Ge coverage and was annealed to 900 K [(a) and (c)], and the other had 0.2-ML Ge coverage and was annealed to 600 K [(b) and (d)]. A schematic diagram of a  $c(2 \times 2)$  overlayer is shown in (e), where open circles represent atoms of the  $1 \times 1$  substrate and shaded circles indicate atoms of the overlayer. The change of the critical angle for enhanced scattering for “open” and closed packed structure is shown schematically in (f). For a structure with a long neighbor separation (left) a smaller critical polar angle is observed than for a densely packed structure (right).

$\sim 1^\circ$  lower for Ge than for Pt scattering. Also, there is no appreciable concentration of Ge in the second layer because there is no Ge-scattering peak observed near  $70^\circ$ . Along the [011] azimuth, observation of a critical polar angle for Ge that is much smaller than for Pt, and thus a Ge nearest neighbor distance that is much larger than that for Pt, further establishes that a  $c(2 \times 2)$ -Ge overlayer is formed. This is shown more clearly in the schematic drawing in Figs. 2(e)

and 2(f). Atomic separations along the [010] azimuth are the same within a  $c(2 \times 2)$  overlayer and the  $1 \times 1$  Pt(100) substrate. However, along the [011] azimuth, Ge-Ge separations in the  $c(2 \times 2)$ -Ge overlayer is twice the Pt-Pt separation in the  $1 \times 1$  Pt(100) substrate and this causes a large decrease in the critical angle for Ge scattering along the [011] azimuth, but not along the [010] azimuth, compared to Pt scattering from the substrate.

The small difference in critical angles for Ge and Pt scattering along the [010] azimuth can have various origins, including defects in the  $c(2 \times 2)$  overlayer that are also observed in STM images (not shown), significantly different backgrounds for the Pt and Ge single-scattering peaks used to construct these plots, or possibly an additional buckling or local displacements of Ge atoms in the  $c(2 \times 2)$  overlayer.

In Figs. 2(b) and 2(d), the critical angles for Pt scattering are the same as those in Figs. 2(a) and 2(c). For Ge scattering, polar scans along the [010] azimuth show a broad feature that extends to angles as low as  $4^\circ$ . This implies that the surface is not uniform, and there is a wide variation in Ge-Ge distances, with some long separations along the [010] azimuth. Along the [011] azimuth, the shift in the Ge-scattering critical angle to lower values confirms a Ge overlayer is produced on this surface also. The broad and weak features, along with additional shifts in the Ge-scattering critical angle compared to that for the  $c(2 \times 2)$ -Ge overlayer, indicates disorder within the adlayer and possibly the occupation of multiple binding sites, e.g., twofold and fourfold sites. The lack of long-range order is consistent with the interpretation of the STM images shown in Fig. 1.

In conclusion, the data presented here show that alloying with the Pt(100) surface is suppressed for low coverages of Ge, i.e., Ge adatoms remain in an overlayer up to quite high temperatures (1200 K). Furthermore, in contrast to previously studied metal-on-metal systems, low coverages of Ge disperse across the surface indicating a repulsive interaction between Ge adatoms. For a 0.5-ML Ge coverage, a  $c(2 \times 2)$ -Ge overlayer forms. Deposition in excess of 0.5-ML Ge and subsequent annealing to 900 K also forms a  $c(2 \times 2)$  overlayer, with excess Ge diffusing deep into the Pt bulk.<sup>21</sup>

Ge and Pt alloy to form bulk intermetallic phases. Also, a dilute surface alloy with Ge incorporated into the surface Pt layer forms readily on Pt(111) at 900 K, with excess Ge diffusing into the bulk.<sup>7,8</sup> Therefore the suppressed alloying of Ge at the Pt(100) surface for low coverages is surprising. Although there is more work required to understanding this phenomenon it must have its origin in an especially deep chemisorption well for Ge adatoms on Pt(100) and the effect of this to force population of adlayer sites prior to alloying. An increased covalent character of the Pt-Ge bonding interaction and the accompanying charge localization may also explain why this system behaves differently than other metal-on-metal systems. Ge can act as an electron acceptor,<sup>24</sup> and thus charge transfer may play an important role in the alloy suppression phenomena and may explain the tendency of Ge to disperse across the surface because of a repulsive dipole-dipole interaction between negatively charged ada-

toms. Because adatoms block reactive sites vastly more efficiently than alloyed atoms, the observation that Ge forms an overlayer on the (100) and not on the (111) face upon annealing allows for the prospect of selectively deactivating (100) facets on Pt nanoclusters in catalysts by Ge additives.

## ACKNOWLEDGMENT

This work was partially supported by the National Science Foundation (NSF), Division of Chemistry, Analytical and Surface Chemistry Program.

---

\*Present address: Department of Physics, Tulane University, New Orleans, LA 70018, USA. Email address: mbatzill@tulane.edu

†Corresponding author. Email address: koel@usc.edu

<sup>1</sup>B. Coq, A. Tijani, and F. Figueras, *J. Mol. Catal.* **71**, 317 (1992).

<sup>2</sup>R. W. Joyner and E. S. Shpiro, *Catal. Lett.* **9**, 239 (1991).

<sup>3</sup>J. Goldwasser, B. Arenas, C. Bolivar, G. Castro, A. Rodriguez, A. Fleitas, and J. Giron, *J. Catal.* **100**, 75 (1986).

<sup>4</sup>A. Borgna, T. F. Garetto, C. R. Apesteguia, and B. Moraweck, *Appl. Catal., A* **182**, 189 (1999).

<sup>5</sup>S. G. Fiddy, M. A. Newton, T. Campbell, J. M. Corker, A. J. Dent, I. Harvey, G. Salvini, S. Turin, and J. Evans, *Chem. Commun.* **2001** (5), 445 (2001).

<sup>6</sup>S. G. Fiddy, M. A. Newton, J. M. Corker, and J. Evans, *J. Phys. Chem. B* **105**, 5244 (2001).

<sup>7</sup>K. Fukutani, Y. Murata, J. Brillo, H. Kuhlenbek, H.-J. Freund, and M. Taguchi, *Surf. Sci.* **464**, 48 (2000).

<sup>8</sup>C.-S. Ho, S. Banerjee, D. Beck, M. Batzill, and B. E. Koel (unpublished).

<sup>9</sup>T. Komatsu, M. Mesuda, and T. Yashima, *Appl. Catal., A* **194**, 333 (2000).

<sup>10</sup>T. Komatsu, S.-I. Hyodo, and T. Yashima, *J. Phys. Chem. B* **101**, 5565 (1997).

<sup>11</sup>K. Fukutani, T. T. Magekoev, Y. Murata, and K. Terakura, *Surf. Sci.* **363**, 185 (1996).

<sup>12</sup>K. Fukutani, T. T. Magekoev, Y. Murata, M. Matsumoto, T.

Kawauchi, T. Magome, Y. Tezuka, and S. Shin, *J. Electron Spectrosc. Relat. Phenom.* **88**, 597 (1998).

<sup>13</sup>L. P. Nielsen, F. Besenbacher, I. Stensgaard, E. Lægsgaard, C. Engdahl, P. Stoltze, K. W. Jacobsen, and J. K. Nørskov, *Phys. Rev. Lett.* **71**, 754 (1993).

<sup>14</sup>H. Röder, R. Schuster, H. Brune, and K. Kern, *Phys. Rev. Lett.* **71**, 2086 (1993).

<sup>15</sup>M. Batzill and B. E. Koel, *Europhys. Lett.* **64**, 70 (2003).

<sup>16</sup>J. Tersoff, *Phys. Rev. Lett.* **74**, 434 (1995).

<sup>17</sup>D. E. Beck, M. Batzill, C. Baur, and B. E. Koel, *Rev. Sci. Instrum.* **73**, 1267 (2002).

<sup>18</sup>Y. Li, M. R. Voss, N. Swami, Y.-L. Tsai, and B. E. Koel, *Phys. Rev. B* **56**, 15982 (1997).

<sup>19</sup>A. Hopkinson, J. M. Bradley, X.-C. Guo, and D. A. King, *Phys. Rev. Lett.* **71**, 1597 (1993).

<sup>20</sup>M. Batzill and B. E. Koel, *Surf. Sci.* **553**, 50 (2004).

<sup>21</sup>T. Matsumoto, M. Batzill, C.-S. Ho, and B. E. Koel (unpublished).

<sup>22</sup>H. Niehus, in *Practical Surface Analysis*, 2nd ed., Ion and Neutral Spectroscopy, Vol. 2, edited by D. Briggs and M. P. Seah (Wiley, Chichester, England, 1992).

<sup>23</sup>Y. Li and B. E. Koel, *Surf. Sci.* **330**, 193 (1995).

<sup>24</sup>T. F. Garetto, A. Borgna, and C. R. Apesteguia, *Stud. Surf. Sci. Catal.: 11th International Congress on Catalysis—40th Anniversary* **101**, 1155 (1996).